17th World Conference on Earthquake Engineering, 17WCEE

Sendai, Japan - September 13th to 18th 2020

SUBSURFACE VELOCITY STRUCTURE BASED ON MICROTOREMOR OBSERVATION IN YURIHAMA TOWN, TOTTORI, JAPAN

I. Nishimura[1], T. Noguchi[2], T. Kagawa[3]

[1] *Graduate student, Tottori University, Graduate School of Sustainability Science, springline23@gmail.com*
[2] *Assistant Professor, Tottori University, Department of engineering, noguchit@tottori-u.ac.jp*
[3] *Professor, Tottori University, Department of engineering, kagawa@tottori-u.ac.jp*

Abstract

An earthquake with M_{JMA} 6.6 occurred in the central part of Tottori Prefecture in Japan on October 21, 2016. Recorded JMA seismic intensity were 6 lower at Kurayoshi city, Yurihama town and Hokuei town. We assumed nonlinear soil response due to strong ground motion at Ryuto and Hisadme observation sites in Yurihama town from the observed data. Housing damages were mainly found at mountain edge more than at flatland. In this study, microtremor observations were carried out around the strong motion observation sites in Yurihama town. Microtremor H/V spectra and their distribution of the predominant period were estimated from the observation data and subsurface velocity structures were estimated using the H/V spectra. It was found that the predominant period at Ryuto is about 0.5-0.8 seconds, and about 1.0-1.5 seconds at Hawai. Predominant period at the edge of mountain was 0.1-0.4 seconds and the periods suspect to housing damages. Results of microtremor array observations are as follows. The maximum thickness of soft soil layer with S-wave velocity from 90m/s to 200m/s is about 60m. This layer becomes thinner towards the edge of the mountain. It was found that there was almost no difference in deeper S-wave velocity structure, and the surface layer was dominant on the site response. The nonlinear ground response in the area might be caused by differences of the subsurface velocity structure down to about 60m depth. The reason why we reached the hypothesis are discussed in the study.

Keywords: microtremor observation, subsurface velocity structure, the 2016 central Tottori earthquake

1. Introduction

On October 21, 2016, an earthquake with M_{JMA} 6.6 occurred in the central part of Tottori Prefecture in Japan. Observed JMA seismic intensity were 6 lower at Kurayoshi city, Yurihama town and Hokuei town (Fig.1). Housing damages occurred mainly in the above areas. Completely destroyed houses were 18 and partially damaged were more than 15,000 [1]. Housing damages in Hokuei town were concentrated in limited areas at the flatland, and at the edge of mountain in Yurihama town [2]. These damages might be caused by site amplification due to differences in subsurface structures.

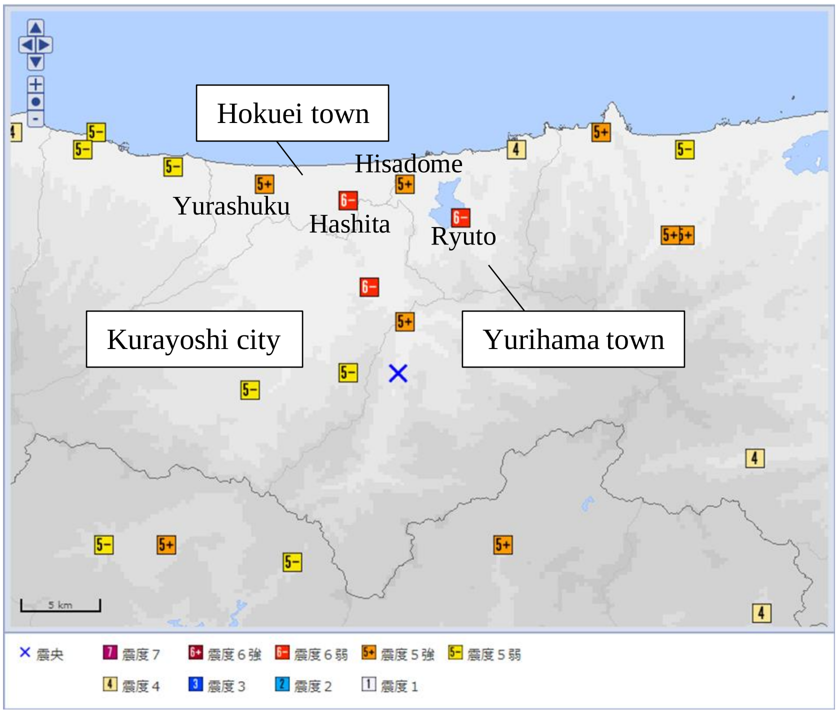

Fig 1 - Seismic intensity distribution of the 2016 Central Tottori Prefecture earthquake[3]

The mainshock and aftershocks had been observed at NIED's K-net and KiK-net, and observation sites of local governments in Tottori Prefecture and temporary sites of Tottori University. There are three local stations and two temporary stations in Yurihama town. From the analysis of these strong motion records [4], variation of site amplifications due to differences in subsurface structure were confirmed. Also, nonlinear soil response due to strong ground motion is suspected at Ryuto and Hisadome observation sites in Yurihama town, and Hashita in Hokuei town [5].

In order to evaluate strong motion, nonlinear soil response, and the relationship between ground motion and damage, it is necessary to understand detailed subsurface structure and ground motion characteristics. In this study, we carried out microtremor observations around the strong motion observation sites and damaged area in Yurihama town, and estimated subsurface structure and ground motion characteristics. In addition, aftershock observations were performed at housing damage area near the mountain foot, and deeper ground structure was estimated from the records.

2. Observation

2.1 Overview of the target area

The topography and geology are as follows [6]. The Kurayoshi plain is formed by sedimentation of the Tenjin River, a first-class river. The west side of the Tenjin River mouth is a coastal sand dune (Hojo Sand Dunes). There is the Togo Pond at the east side of the river. Alluvial lowlands (Kurayoshi Plain at coastal area) with soft sand and clay are spreading in the area. Paleogene rhyolite and granite, Neogene andesite and basalt are found in the surrounding mountains that form the base of the plain. Sand layers from Hojo Sand Dunes are found in the west side of Togo Pond. The northwest side of Togo Pond is called Hawai region, and the southeast side is called Togo region.

Housing damage due to the mainshock of the 2016 earthquake was concentrated in the mountainside in Yurihama town. In the damaged area shown in Fig. 2, roof tile damage was estimated based on the blue sheet coverage from the satellite image [7], and confirmed by site visits and interviews. In this study, an area with 50m radius from the damaged houses was considered as the housing damage area.

According to previous study [8], the predominant period of microtremor around Togo Pond is about 0.5-1.5 seconds. The predominant period increases from the southeastern mountains area to the northwestern coast. It is considered to correspond to thickness of soft layer with S-wave velocities 100-200 m/s.

2.2 Summary of observation

Single-point observations were carried out at 112 sites around Hisadome and 80 sites around Ryuto, mainly in residential areas and strong motion observation sites around Togo Pond. In Oshikadani and Takatsuji with the roof tiles damage, we observed 102 sites at 50 m intervals. The equipment used was JU410, a three-component accelerometer. The specifications used amplification factor 100, sampling frequency 100 Hz or 200 Hz, and observation time about 10-15 minutes.

Array observations were conducted at nine sites: two strong motion observation sites (YRAR, TGAR), two temporary aftershock observation sites (OSK, TZAR), and five other residential areas. Four JU410 synchronized with the GPS clock were used for the measurement. One seismometer was placed at the center of the circle and other three were placed around the circumference to form an equilateral triangle. The sampling frequency was 200 Hz, the amplification factor was in the same way as for single-point observation, and the observation time was about 15 minutes. The array radius was set within the range of 0.6 to 30 m, depending on the observation site, to evaluate S-wave velocity structures of Quaternary sediments.

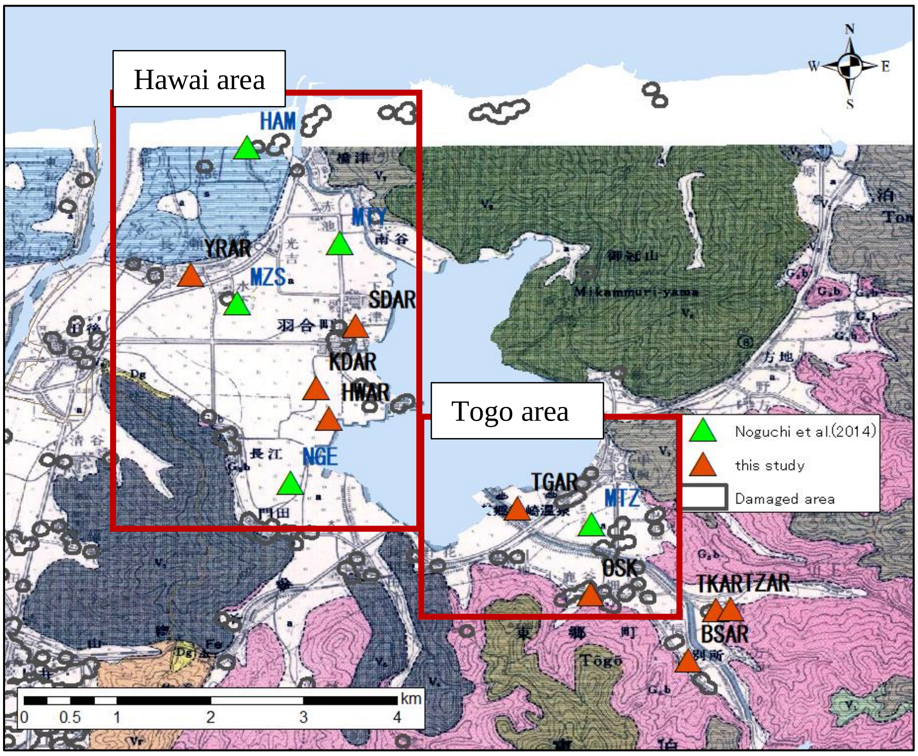

Fig 2 - Damaged area and Array observation sites in Yurihama town

Aftershock observations were placed at Oshikadani and Takatsuji (OSK, TZAR) where the houses were damaged. Oshikadani site has been maintained from July 24, 2017 to July 2, 2018, and Takatsuji site is working from October 20, 2015. The observation equipment was used a sensor integrated recorder CV-374A, and the sampling frequency was 100 Hz. The seismometers were installed indoors on a solid foundation, such as at the entrance of a building where external power can be secured.

3. Analysis

3.1 Microtremor records

From a single-point observation record, Fourier spectrum was calculated, and smoothed using a Log window with a coefficient of 20 [9]. Average spectrum was calculated from at least 10 stable 20.48 second sections. From the Fourier spectra, the horizontal to vertical spectral ratio (H/V) was calculated, and predominant period and peak value (amplitude ratio) were visually estimated. Many H/V were unimodal with a single distinct peak. In some areas such as mountainside where multiple peaks were observed, the predominant period was estimated in consideration of continuity with adjacent unimodal sites. Fig. 3 shows the entire predominant period distribution map in Yurihama town, Fig. 4 and 5 show Oshikadani and Takatsuji regions respectively.

In the analysis of array observation, the analysis including the past research data [8] was performed in order to unify the velocity structure of the lowermost surface. The analysis method is as follows. Using the published analysis tool [10], the phase velocity dispersion curve of the array observation record was estimated based on the CCA method [11]. As analysis specifications, at least five sections were selected by automatic extraction using RMS values of microtremor recordings with 10.24 seconds segments. Next, power spectra in

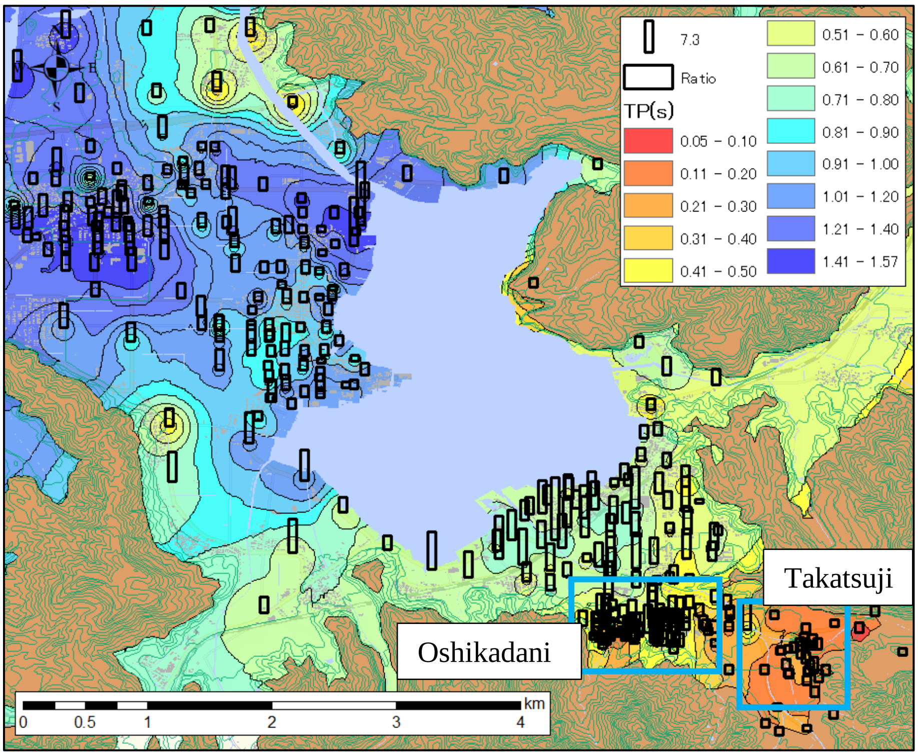

Fig 3 - Predominant period and peak value (rectangular length) in Yurihama town

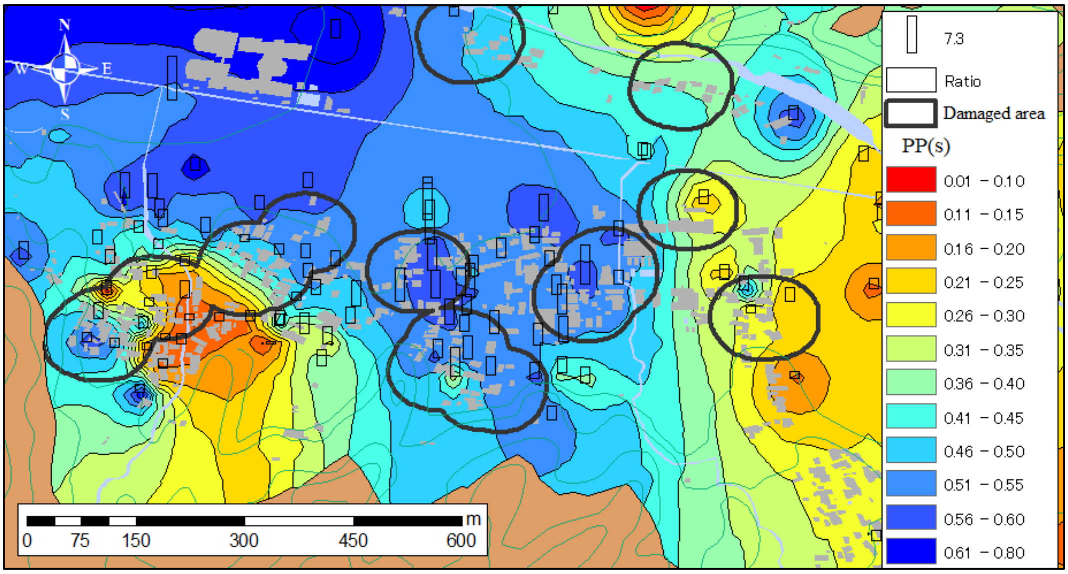

Fig 4 - Predominant period and peak value (rectangular length) distribution in Oshikadani region

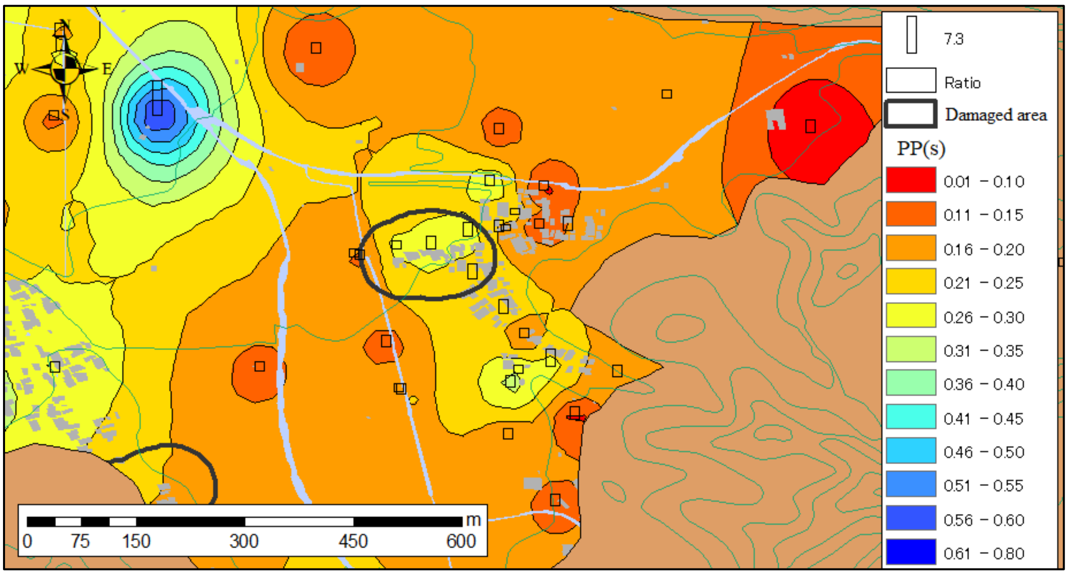

Fig 5 - Predominant period and peak value (rectangular length) distribution in Takatsuji region

those sections were smoothed with 0.3 Hz bandwidth Parzen window, and averaged, finally phase velocity dispersion curve was determined. The phase velocity dispersion curves obtained at each radius were summarized at each observation site considering continuity.

Using the phase velocity dispersion curve and the microtremor H/V obtained from the single-point microtremor recording at the center of array, subsurface structure model was estimated by forward modeling based on the fundamental mode of Rayleigh waves. The S-wave velocity was determined with reference to previous research [8] and borehole data [12]. Then modeling was performed by changing the layer thickness. Density was set referring previous research [8], and P-wave velocity was set from S-wave velocity [13]. Table 1 shows the resulting subsurface structure model. Appendix fig. 1 shows the microtremor H/V at the center of the array observation site, superposed with the theoretical value based on the model in Table 1.

3.2 Aftershock records

From the records of 15 earthquakes that occurred between July 24, 2017 and July 2, 2018, the simultaneously observed earthquakes at the both sites were analyzed. Time windows of 10.24 seconds were extracted from the S-wave arrival, and cosine tapers were applied to 5% of both ends. After that, the time window was prolonged to 20.48 seconds added with zero data, and Fourier spectrum was calculated by smoothing with 0.2 Hz bandwidth Parzen window. From the Fourier spectrum of each component, the spectral ratio of the horizontal to vertical (strong ground motion H/V) was evaluated.

Table 1 – Subsurface structure model based on array observation

(Site locations are shown in Fig.2.)

Site	Thickness(m)	ρ (t/m^3)	Vp(m/s)	Vs(m/s)	Site	Thickness(m)	ρ (t/m^3)	Vp(m/s)	Vs(m/s)
YRAR	33	1.6	1430	140	TGAR	9	1.6	1390	90
	75	1.8	1730	400		8	1.7	1510	200
	100	2.1	2070	700		50	1.8	1730	400
	∞	2.2	2620	1200		100	2.1	2070	700
HAM	27	1.7	1510	200		∞	2.2	2620	1200
	20	1.8	1730	400	MTZ	3	1.6	1400	100
	100	2.1	2070	700		17	1.7	1510	200
	∞	2.2	2620	1200		30	1.8	1730	400
MZS	33	1.6	1430	140		100	2.1	2070	700
	75	1.8	1730	400		∞	2.2	2620	1200
	100	2.1	2070	700	OSKAR	8	1.6	1400	100
	∞	2.2	2620	1200		3	1.7	1510	200
MTY	40	1.6	1430	140		30	1.8	1730	400
	40	1.8	1730	400		100	2.1	2070	700
	100	2.1	2070	700		∞	2.2	2620	1200
	∞	2.2	2620	1200	TKAR	13	1.7	1480	160
SDAR	40	1.6	1430	140		100	2.1	2070	700
	40	1.8	1730	400		∞	2.2	2620	1200
	100	2.1	2070	700	TZAR	4	1.6	1390	100
	∞	2.2	2620	1200		4	1.7	1510	200
KDAR	13	1.6	1400	100		100	2.1	2070	700
	45	1.8	1730	400		∞	2.2	2620	1200
	100	2.1	2070	700	BSAR	6	1.6	1450	140
	∞	2.2	2620	1200		25	1.8	1730	400
HWAR	23	1.6	1400	100		100	2.1	2070	700
	40	1.8	1730	400		∞	2.2	2620	1200
	100	2.1	2070	700					
	∞	2.2	2620	1200					
NGE	24	1.6	1400	100					
	100	2.1	2070	700					
	∞	2.2	2620	1200					

The subsurface structure model, were estimated by forward modeling at first, modifying the model by comparing the theoretical H/V based on the diffuse wave field theory [14] of strong ground motion H/V. As an initial model the shallow structure was estimated based on the array observation model described above, and the deep structure was estimated from previous research [15]. Furthermore, based on the model, a final structure model was obtained from inversion by a hybrid heuristic search method [16] with genetic algorithm (GA) and simulated annealing (SA). The damping constant h is assumed to be 0.03 for S-wave velocities of 100 m/s or less, 0.02 for 100-400 m/s, and 0.01 for 400 m/s or more.

The settings for inversion parameters are as follows. For GA, the number of trials was 10, the number of samples was 30, the number of generations was 300, the crossover probability was 0.7, the mutation probability was 0.01, and dynamic mutation and elite selection were considered. For SA, the temperature drop function was e.q.(1), with coefficients a 0.5, c 1.0, initial temperature T_0 100, and number of temperature updates 10.

The S-wave velocity and layer thickness of the first layer and the bottom layer were fixed, and the other layers were searched within a range of ± 25% from the initial value. The search targets were the S-wave and P-wave velocities and the layer thickness. Density was obtained from the conversion formula [17] from S-wave velocity. Appendix fig. 2 shows a comparison between the observed strong ground motion H/V and the theoretical H/V calculated from estimated model, and Table 2 shows the resulting ground parameters from shallow to deep layers.

$$T = T_0 \exp(-ck^a) \quad (1)$$

Table 2 - Subsurface structure models based on seismic motion analysis

Oshikadani

Thickness(m)	ρ (t/m^3)	Vp(m/s)	Vs(m/s)	h
5.0	1.60	1390	90	0.03
42.8	1.82	1717	384	0.02
52.1	2.07	2394	995	0.01
338.6	2.11	2527	1114	0.01
317.0	2.28	3209	1729	0.01
∞	2.56	5500	3000	0.01

Takatsuji

Thickness(m)	ρ (t/m^3)	Vp(m/s)	Vs(m/s)	h
6.0	1.60	1390	90	0.03
5.4	1.71	1535	212	0.02
83.3	1.94	2001	627	0.01
162.4	2.13	2605	1191	0.01
194.0	2.31	3323	1867	0.01
∞	2.56	5500	3000	0.01

4. Discussions

4.1 Predominant period of microtremor H/V

The predominant period distribution is as follows. The predominant period in Fig.3 is 0.8-1.6 seconds on the northwest side of Togo Pond and 0.4-0.8 seconds on the southeast side. In Oshikadani and Takatsuji located near the mountainsides, the predominant period is 0.1-0.4 seconds. The peak value is low in the coastal area and the lakeside of Togo Pond in Hawai area, and in the area near the mountainsides. The peak value tends to be high in the plain.

Oshikadani and Takatsuji regions are areas where housing damages were reported, and dense observations were carried out. From Fig. 4, the predominant period is 0.4-0.6 seconds in the central part of Oshikadani, and shorter than 0.4 seconds in the east and west parts. The peak value tends to be large in the center and smaller in the west and east parts. As shown in Fig. 5, the predominant period is 0.1-0.4 seconds, and the peak value tends to be small overall in Takatsuji. From Fig.4 and Fig.5, the distribution of housing damage is widespread in Oshikadani and concentrated in Takatsuji. Unfortunately, clear relationship is not found between the distribution of building damage and the predominant period distribution in both areas.

4.2 Estimation of subsurface structure

From the borehole data around Togo Pond [12], S-wave velocity of 100 m/s or less in Table 1 is considered to be clay or silt layer, and S-wave velocity of 200-300 m/s is considered to be sand layer. Table 1 shows that the thickness of the layer with S-wave velocity of 90-300 m/s is 6-75m at each site. The low velocity layer with S-wave velocity less than 200 m/s tends to be thicker around Togo Pond and thinner depth to inland. In Takatsuji, a layer with S-wave velocity of 200 m/s was piled up from the surface to about 10m depth, a solid bedrock layer with S-wave velocity of 700 m/s is estimated below that. In Oshikadani, thickness of the S-wave velocity of 400 m/s or less is about 40m, which is 4 times thicker than those in Takatsuji. It was found that there was a silt layer with S-wave velocity of 140 m/s in the surface layer at Hisadome (YRAR) and a layer with 90 m/s S-wave velocity in the surface layer of Ryuto (TGAR). It is suggested that the silt layer caused nonlinear response in both areas.

At the two observation sites near the mountainside, a deeper subsurface structure model was estimated from aftershock observation records. Table 2 shows that the deep layers with S-wave velocity of 1000 m/s or more, is thinner in Takatsuji than Oshikadani for all layers. Therefore, it is suggested that the shaking was different at both sites because of the deep structures due to the mainshock.

5. Conclusion

Microtremor surveys were carried out in Yurihama town, Tottori Prefecture, and the subsurface structure was estimated using data from previous studies and this study. In conclusion, the following results were found.

a) H/V obtained from the single-point observation of microtremor tended to have a longer predominant period in the mountainside than the plain. The peak values tended to be smaller at the lakeside in Hawai and at the mountainside areas in Oshikadani and Takatsuji.

b) The phase velocity dispersion curve was obtained from the microtremor array observation record, and the S-wave velocity structure was estimated from them. The low-velocity layer with S-wave velocity less than 200 m/s tended to be thicker in the plain around Togo Pond and thinner in the inland. In Hisadome and Ryuto where nonlinear response was observed, low velocity silt layers were found in the surface layer, and it is highly suspected that the layer affected in nonlinear response in the area.

c) A deeper subsurface structure model in Oshikadani and Takatsuji was estimated from aftershock observation records. As a result, it was found that the layers in Oshikadani are thicker than Takatsuji. It might affect the mainshock that causes different damages in the areas.

Furthermore, we are planning to carry out detailed ground response analysis based on the subsurface structure models for strong motion evaluation in the area.

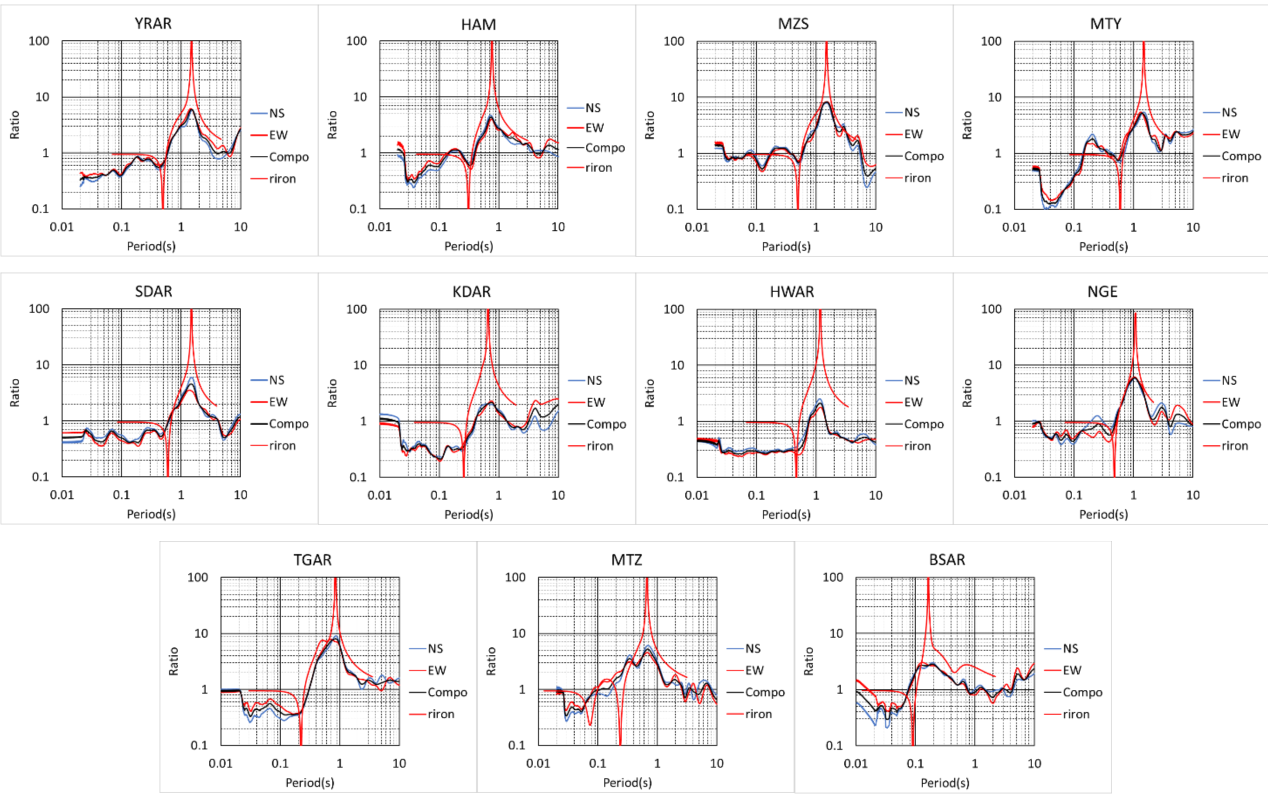

Appendix fig 1(a) - Microtremor H/V at array observation sites

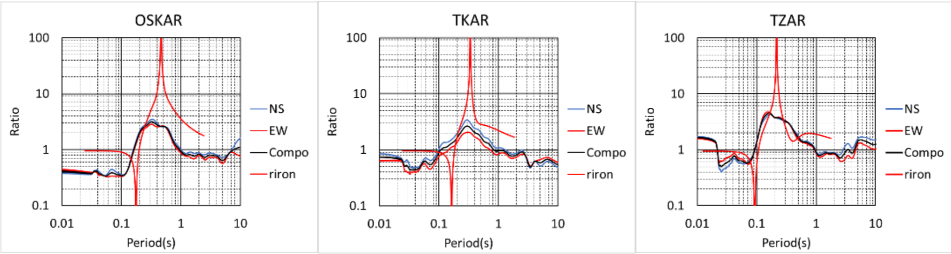

Appendix fig 1(b) - Microtremor H/V at array observation sites

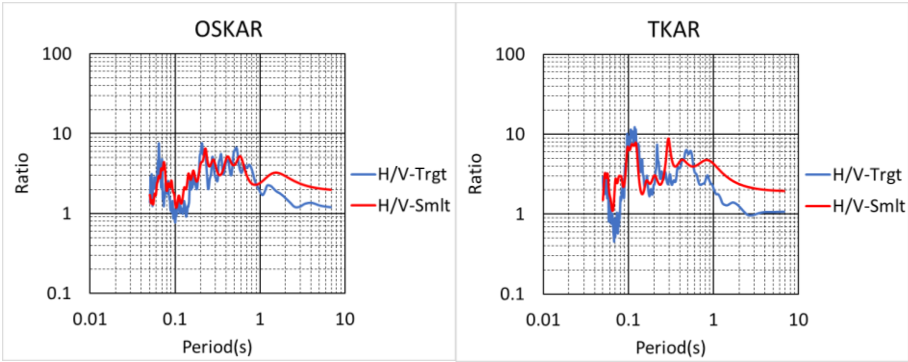

Appendix fig 2 – Comparison between observed and synthesized H/V of strong ground motion

(blue line: strong ground motion H/V, orange line: theoretical H/V)

Acknowledgements

In this study, the microtremor observation was supported by students from the Geosphere Environmental Engineering Laboratory, Faculty of Engineering, Tottori University. For the calculation of the inversion, we used the program source by Dr. Yuzuru Yasui. Mr. Ichihashi, a member of volunteer fire department in the local government, and Mr. Yamamoto, a technical staff member of the Faculty of Engineering, Tottori University, cooperated in setting up observation sites at Oshikadani and Takatsuji, collecting data, and reporting the local damages. We appreciate to everyone who supported.

References

[1] Tottori Prefecture (2018): The earthquake in central Tottori Prefecture (100th report) (March 20, 12:00), <https://www.pref.tottori.lg.jp/secure/1114702/100.pdf>, [Viewed on August 23, 2019].

[2] Kagawa, T. (2017): 2016 Central Tottori Earthquake (M6.6), Earthquake Journal, No.63, pp.14-22.

[3] Japan Meteorological Agency: Seismic intensity database, <https://www.data.jma.go.jp/svd/eqdb/data/shindo/Event.php?ID=202792>, [Viewed on August 24, 2019].

[4] Noguchi, T., Nishikawa, H., Yoshida, S. and Kagawa, T. (2019): Estimation of subsurface structure and characteristics of ground vibration based on microtremor and seismic observation in the central Tottori Prefecture (in Japanese), Japan, Journal of Japan Association for Earthquake Engineering, Vol. 19, Issue 6, pp 258-271.

[5] Noguchi, T., Nishikawa, H., Kagawa, T. and Yoshida, S. (2018): Nonlinear soil response due to the 2016 central Tottori earthquake (in Japanese), JSCE Journal of Earthquake Engineering, Vol.37, pp1010-1016.

[6] Geological Survey (1982): 1: 200,000 Geological Map "Matsue and Taisha".

[7] Honda, Y., Mochizuki, K., Shimomura, H. and Monma, N. (2017): Automatic extraction of blue sheet-covered housing from satellite images of 2016 Central Tottori Earthquake (in Japanese), Japan Society for Disaster Information Studies, Proceedings of the 19th conference, pp.244-245.

[8] Noguchi, T., Kagawa, T. (2014): Determination of subsurface structure of the seaside area of Kurayoshi Plain (in Japanese), Tottori Prefecture by microtremor and gravity exploration, JSCE Journal of Earthquake Engineering, Vol.33, pp.888-896.

[9] Konno, K., Ohmachi, T. (1995): A smoothing function suitable for estimation of amplification factor of the surface ground from microtremor and its application (in Japanese), Transactions of the Japan Society of Civil Engineers, No525/I-33, pp247-259.

[10] Cho, I., Tada, T. and Shinozaki Y. (2009): Possibility of microtremor array opened up by general theory :Release of analysis tool BIDO, Seismological Society of Japan Fall Meeting in 2009.

[11] Cho, I., Tada T. and Shinozaki Y. (2006): Centerless circular array method: Inferring phase velocities of Rayleigh waves in broad wavelength ranges using microtremor records, J. Geophys. Res., 111, B09315.

[12] National Research Institute for Earth Science and Disaster Resilience: Geo Station, <https://www.geo-stn.bosai.go.jp/>, [Viewed on October 9, 2019].

[13] Kitsunezaki, C., Goto, N., Kobayashi, Y., Ikawa, T., Horike, M., Saito, T., Kurota, T., Yamane, K., Okuzumi, K. (1990): Estimation of P- and S- wave velocities in deep soil deposits for evaluating ground vibrations in earthquake (in Japanese), Natural disaster science, 9-3, 1-17.

[14] Kawase, H., Sanchez-Seama, F.J. and Matsushima, S. (2011): The optimal use of horizontal-to-vertiacal spectral ratios of earthquake motions for plane waves, Bull. Seism. Soc. Am. Vol.101, No.5, pp.2001-2014.

[15] Noguchi, T., Nishikawa, H., Yoshida, S. and Kagawa, T. (2016): Subsurface structure and evaluation of site effects at strong ground motion observation sites in Tottori Prefecture (in Japanese), JSCE Journal of Earthquake Engineering, Vol.72, Issue 35, pp.646-658.

[16] Yamanaka, H. (2007): Inversion of surface-wave phase velocity using hybrid heuristic search method (in Japanese), Geophysical Exploration, Vol. 60, Issue 3, pp-265-275.

[17] Ota, T., Emori, K. and Kasai, Y. (2001): Building foundation earthquake resistance / vibration / control, Kyoritsu Shuppan, pp-339.

